

1 **MyROOT: A novel method and software for the semi-automatic measurement of**
2 **plant root length**

3

4 **Authors: Isabel Betegón-Putze^{1,*}, Alejandro González^{2,*}, Xavier Sevillano², David**
5 **Blasco-Escámez¹ and Ana I. Caño-Delgado^{1, †}**

6

7

8 **Affiliations:**

9 ¹*Department of Molecular Genetics, Center for Research in Agricultural Genomics (CRAG)*
10 *CSIC-IRTA-UAB-UB, Campus UAB, Bellaterra (Cerdanyola del Vallès), 08193 Barcelona,*
11 *Spain.*

12 ²*GTM- Grup de recerca en Tecnologies Mèdia, La Salle, Universitat Ramon Llull, 08022*
13 *Barcelona, Spain.*

14 *equal author contribution

15 †Correspondence to: ana.cano@cragenomica.es

16 Present address:

17 Dept. Molecular Genetics

18 Centre de Recerca en Agrigenòmica (CRAG) CSIC-IRTA-UAB-UB

19 Campus UAB, Bellaterra (Cerdanyola del Vallés)

20 E-08193 Barcelona, Spain

21 Tel: +34 93 563 66 00 ext. 3210

22 Fax: +34 93 563 66 01

23 <http://canolab.cragenomica.es/>

24

25

26

27

28 **ABSTRACT**

29 Root analysis is essential for both academic and agricultural research. Despite the great
30 advances in root phenotyping and imaging however, calculating root length is still
31 performed manually and involves considerable amounts of labor and time. To overcome
32 these limitations, we have developed MyROOT, a novel software for the semi-automatic
33 quantification of root growth of seedlings growing directly in agar plates. Our method
34 automatically determines the scale from the image of the plate, and subsequently
35 measures the root length of the individual plants. To this aim, MyROOT combines a
36 bottom-up root tracking approach with a hypocotyl detection algorithm. At the same time
37 as providing accurate root measurements, MyROOT also significantly minimizes the user
38 intervention required during the process. Using *Arabidopsis*, we tested MyROOT with
39 seedlings from different growth stages. Upon comparing the data obtained using this
40 software with that of manual root measurements, we found that there are no significant
41 differences (t-test, p-value < 0.05). Thus, MyROOT will be of great aid to the plant
42 science community by permitting high-throughput root length measurements while
43 saving on both labor and time.

44

45 **INTRODUCTION**

46 The root, which is responsible for anchoring the plant to the soil, is an essential organ for
47 overall plant growth and development. The characterization of different root traits is
48 therefore important not only for understanding organ growth, but also for evaluating the
49 impact of roots in agriculture ¹. As such, generating tools for precise, high-throughput
50 phenotyping and imaging of the root is essential for plant research and agriculture. Even
51 phenotyping facilities such as the ones available in the European Plant Phenotypic
52 Network (<http://www.plant-phenotyping-network.eu/>) have started to implement tools for
53 the massive screening of roots.

54 Roots provide the necessary structural and functional support for the incorporation of
55 nutrients and water from the soil. In *Arabidopsis thaliana* (*Arabidopsis*), the primary root
56 has a very simplified anatomy that makes it very amenable for genetic and microscopic
57 analyses ²⁻⁴. Different root cell lineages are derived from the activity of a group of stem
58 cells located at the root apex. Here, the stem cell niche is formed by a few (3-7) quiescent
59 center (QC) cells that occasionally divide asymmetrically to renew themselves and to

60 form daughter stem cells. From the root apex, these cells actively divide in the
61 meristematic zone, and before exiting the cell cycle in the transition zone, continue to
62 elongate and differentiate in spatially separated regions of the root. In this way, primary
63 root growth is determined by the balance between cell division and cell elongation within
64 the different zones of the root⁵⁻⁸.

65 The most straightforward symptom of abnormal root growth or development can be
66 identified by examining the length of the primary root in seedlings. Abnormalities in
67 length can usually be observed and measured just five to six days after germination
68 (DAG), where still reflect their embryonic origin⁹. Growth defects in the primary root of
69 seedlings are not only consistent with overall growth defects, but also persistent along the
70 entire plant life cycle¹⁰⁻¹². Indeed, Arabidopsis root analyses were the foundations for
71 multiple genetic screens that ultimately led to the identification of several key regulators
72 of plant growth and development^{10,13-16}.

73 Root analysis of young seedlings offers direct information regarding overall plant growth
74 and viability. Despite important advances in plant imaging techniques such as
75 microscopic visualization¹⁷⁻¹⁹, the root length of seedlings growing in agar plates is
76 generally measured by manually indicating the position of each seedling or manually
77 tracking each root using the ImageJ software (<https://imagej.nih.gov/ij/>). For this reason,
78 the development and use of methods that enable the automatic analysis of a large number
79 of roots represents a step forward for high-throughput root analysis. Automatic analysis
80 of root system architecture is just beginning to be implemented, and novel methods based
81 on acquiring, processing, and obtaining quantitative data from root images are now
82 available (for a review, see¹⁹).

83 With this in mind, our rational was to develop MyROOT, a software capable of semi-
84 automatically calculating root length. By precisely detecting all individual roots and
85 hypocotyls growing on an agar plate from a JPEG image, this software simplifies and
86 minimizes user intervention during the calculation of root length. As a proof of concept,
87 MyROOT software was first used for root length measurement of wild type and
88 brassinosteroid-signaling Arabidopsis mutants grown in control and osmotic stress
89 conditions. MyROOT software is available at [https://www.cragenomica.es/research-](https://www.cragenomica.es/research-groups/brassinosteroid-signaling-in-plant-development)
90 [groups/brassinosteroid-signaling-in-plant-development](https://www.cragenomica.es/research-groups/brassinosteroid-signaling-in-plant-development).

91 Currently, a myriad of software is available for measuring root phenotypic traits. These
92 differ with respect to: i) the medium in which the plant is grown, ii) the use of 2D or 3D
93 imaging, iii) the imaging modality, and iv) the degree of manual intervention required
94 from the user ¹. Specifically, when using these available software tools to measure root
95 length, plant scientists face three main hurdles: i) the constraints imposed during the
96 image acquisition process, ii) the ease of use (often related to the degree of manual
97 intervention required), and iii) the accuracy of the root length measurements.

98 Regarding the complexity of the image acquisition process, software tools such as
99 PlaRoM ²⁰ require scanning the plates using a camera-microscope unit mounted on a
100 robotic arm, BRAT ²¹ requires a cluster of several flatbed scanners, and the
101 RootReader2D software ²² requires a camera equipped with two cross-polarized filters.
102 In comparison, MyROOT operates on photographs (of Petri dishes) taken directly from
103 above with a standard digital camera or even a good quality cell phone.

104 In terms of manual intervention, some of the software tools require intensive user
105 participation in order to define certain aspects of the individual roots under analysis. This
106 makes measuring root length a time-consuming and burdensome process. A prime
107 example of this is RootTrace ²³, a software for which the user has to manually define the
108 start point of each root. In contrast, MyROOT merely requires the user to define the region
109 in which the seedlings are placed on the plate, and then subsequently operates in a fully
110 automatic fashion. Moreover, the interactive interface of MyROOT permits the
111 visualization of results from each intermediate step of the root measurement process. In
112 this way, the user can modify any configuration parameter at will, and redo any of the
113 steps if deemed necessary.

114 Finally, as far as measurement accuracy is concerned, the precise detection of root start
115 and end points is critical. While some software tools rely on intensive manual labor for
116 defining the aforementioned points ²⁴, others such as BRAT ²¹ use shoot detection to
117 determine the root start point. In contrast, to ensure that roots are measured correctly from
118 their tip to their true start point, MyROOT combines a bottom-up root tracking approach
119 with a hypocotyl detection algorithm to provide accurate measurements.

120 In summary, not only is MyROOT very straightforward to use, but it can also accurately
121 measure root length on a plate while sparing important and unnecessary human labor.

122

123 **RESULTS**

124 **MyROOT is a software for the high-throughput analysis of root length**

125 The majority of root studies begin with an overall determination of root growth as
126 estimated by manual, laborious and time-consuming measurements. To address this
127 limitation, we developed a semi-automatic and non-invasive software for the high-
128 throughput measurement of root length. This method is implemented in Matlab as an
129 automatic tool named MyROOT (Fig. 1a). It is based on pictures of whole agar plates
130 where young seedlings are growing vertically on the surface, and implements novel
131 algorithms capable of separately detecting the root and the hypocotyl of each individual
132 seedling and estimating a hypocotyl curve based on the detection of some hypocotyls
133 (Fig. 1b-g).

134 MyROOT detects and measures root length by following a series of steps (Fig. 1b-g).
135 First, a digital image of the plate containing the growing seedlings is taken and used for
136 the analysis (Fig. 1b and Fig. S1). The image is taken with a ruler (at least 1 cm long)
137 placed on top of the plate. From each JPEG image, the software: i) detects 1 cm of the
138 ruler to automatically compute the scale and calculate the equivalence between pixels and
139 millimeters (mm; Fig. 1c); ii) generates a binary mask from the manually selected area
140 that allows for root segmentation (this separates those pixels that belong to a root from
141 those of the background) (Fig. 1d); iii) measures the length of the roots through a root
142 tracking process (Fig. 1e); iv) computes a regression curve based on the detection of the
143 hypocotyls to identify the starting point of each root (Fig. 1f); v) measures the root length
144 again from the root tip to the end of the hypocotyl (Fig. 1g); and vi) exports the
145 measurements and the generated masks to a new folder. Finally, the results are saved in:
146 i) an Excel spreadsheet or a TXT file in which each root is identified by an ID tag, length
147 value and a descriptive text label introduced by the user; ii) an image showing the detected
148 and measured roots; and iii) MATLAB variables including the intermediate data such as
149 hypocotyl position and the detection curve that were generated while quantifying root
150 length.

151 One of the advantages of this software is that it allows the user to supervise the different
152 steps of the process as the results of each step are displayed before executing the following
153 one. This feature enables the user to modify the different parameters (e.g., segmentation
154 thresholds for ruler and root detection, and model for hypocotyl detection, etc.) at any

155 point in the process to take into account different image conditions. Nonetheless, default
156 parameter values have been set for satisfactory operation on a wide range of images for
157 pre-defined acquisition conditions (see Material and Methods). Furthermore, the position
158 of any hypocotyl that is not automatically detected can be manually indicated, and
159 undesired roots can be manually removed from the results before saving.

160 In summary, by determining the pixel-millimeter equivalence and detecting seedling
161 morphology (roots and hypocotyls) from an image of a seedling-containing agar plate,
162 MyROOT offers a valuable analytical tool for precisely measuring root growth in a semi-
163 automatic manner. As such, this software clearly provides a solution to the timely task of
164 manually quantifying root length.

165 **Root detection and measurement process**

166 MyROOT has been developed for the high-throughput, accurate, and non-invasive
167 measurement of root length from seedlings growing in agar plates. In this respect, the
168 three most crucial steps are to precisely determine the scale, identify the roots, and
169 measure their length. The scale information is obtained from a piece of measuring tape
170 that is placed on the surface of the Petri dish. This allows the measurements to be
171 completely independent from the specific characteristics of the image capture system.
172 The first step for detecting the ruler is based on its color contrast with the background.
173 By computing the vertical and horizontal profiles of the image, the algorithm is designed
174 to explore the entire image in search of a white patch (Fig. 2a). As the border of the plate
175 has a similar color contrast with the background, a median filter is applied to reduce the
176 border effect. The maximum values in the filtered profiles define the image area where
177 the white patch is present. Next, the resulting area is further cropped (Fig. 2b) and
178 processed (Fig. 2c-e). By applying a threshold based on Otsu's algorithm ²⁵, the black
179 lines representing cm and mm marks are not filtered out (Fig. 2b). Finally, a horizontal
180 profile of this binary image is generated (Fig. 2d) in which the pixel-mm equivalence is
181 defined as the difference between consecutive local maxima (Fig. 2e).

182 The core of the whole method is the root extraction and measurement process. In order to
183 extract roots, the user must first manually define the area in which roots are present (note:
184 only one row of seedlings should be included when defining the area). Then, with just a
185 few mouse clicks from the user, a binary mask is generated that allows root segmentation.
186 This later leads to the identification of individual roots through a root tracking process,

187 and finally allows the individually identified roots to be measured (Fig. 3). The root
188 segmentation process can be divided into four main steps: i) color normalization (Fig.
189 3a), ii) ridge detection (Fig. 3b), iii) root tracking (Fig. 3c), and iv) root identification
190 (Fig. 3d). During the color normalization step, the image is processed and a global
191 working framework is set (i.e., all images going through this process become color-
192 balanced and have the same lower and higher white values; Fig. 3a). This allows the user
193 to manage different initial conditions (illumination, color, and saturation, etc.) while
194 continuing with the same subsequent steps of the pipeline. In the next step, a ridge (i.e.,
195 white contrasted area) detector identifies roots based on their contrast with the
196 background (for this, the level of whiteness is irrelevant; Fig. 3b). After the detection step,
197 a final mask is generated for tracking the roots. Due to the linear disposition of the roots
198 in the plate, we employed a bottom-up tracking approach. As such, tracking starts at the
199 end point of each root and continues upward, row by row, until the hypocotyl detection
200 curve is found (Fig. 3c). Finally, the tracking of each root makes it possible to identify
201 which pixels correspond to which root (Fig. 3d).

202 Once the root tracking process has been completed, each individual root is measured
203 based on previous positions saved in the historical record. Specifically, root length is
204 calculated in pixels by adding the distances between previous consecutive points and then
205 applying the previously calculated pixel-mm equivalence. Next, a refinement process is
206 applied in which very short roots, which are often associated with noise, are discarded.
207 By default, MyROOT discards any root measurement shorter than 30% of the longest
208 one. However, this percentage can be manually chosen by the user if need be. A second
209 filter is then applied in order to keep those roots that terminate close to the previously
210 calculated hypocotyl curve. If a root surpasses the hypocotyl curve, it is cut at this level.
211 Finally, a unique numeric identifier (ID) is assigned to all roots that are not filtered out
212 during processing.

213 As two roots can be located so close to one another that they cannot be detected as
214 individual roots, we trained MyROOT with the following characteristics: i) when a split
215 occurs and a current root matches more than one detection (blue circle in Fig. 3C), a new
216 root sharing the same historical record is created, and ii) when a fusion occurs and two
217 roots match a single detection (yellow circle in Fig. 3c), the shortest root is eliminated
218 from the root set and added as a sub-root of the longest one.

219 To validate our software, we compared root length measurements obtained using
220 MyROOT with manual measurements performed using ImageJ. As a first comparison,
221 six-day-old seedlings grown in three different vertical Petri dishes (n=89) were measured
222 by three different scientists (Fig. 4a). Upon comparing these MyROOT and ImageJ
223 measurements, we observed no significant difference (t-test, p-value < 0.05) in the mean
224 root lengths (23.45, 23.61 and 23.62 mm using ImageJ, and 23.47, 23.51 and 23.35 mm
225 using MyROOT). Taken together, these results indicate that measurements made using
226 our software coincide with manual measurements, thereby supporting the use of
227 MyROOT for root length analysis. Furthermore, a second comparison was conducted by
228 measuring the root length of the same seedlings during six consecutive days (from three
229 to eight DAG; n>116; Fig. 4b). Again, highly similar values were obtained between the
230 MyROOT and manual measurements. Importantly, this validates MyROOT for analyzing
231 the root length of Arabidopsis seedlings at different days after germination.

232 In addition, we also evaluated the time required by MyROOT to determine root lengths,
233 and compared it to the time needed for manual measurements. Importantly, we found that
234 our software significantly reduces the necessary time. MyROOT reduces the time
235 required to measure one plate by approximately half (Fig. S2).

236 **Hypocotyl detection**

237 One of the main advantages of MyROOT is its ability to identify the hypocotyls of the
238 growing seedlings. This characteristic is important for accurately determining the start
239 point of each root. The hypocotyl detection process is based on visual features extracted
240 (appearance and color) from the image. These features were used to generate a hypocotyl
241 model by introducing 1,259 hypocotyls of seedlings of different ages and characteristics
242 and 7,915 samples with background information (see Material and Methods). The learned
243 model is able to determine whether a given sample is a hypocotyl or not. To extract visual
244 features, we implemented the histogram of oriented gradient (HOG) ²⁶ method. The HOG
245 method is based on the orientation of the contours in the image, and generates a histogram
246 that represents the appearance/shape of the sample. For extracting color features, color
247 distribution histograms representing the amount of color in a given sample area are used
248 (Fig. 5a). To train the model, we implemented a linear support vector machine classifier
249 that uses appearance and color features from the hypocotyl images. This classifier
250 generates the best hyperplane that classifies samples as positive (hypocotyls) and negative

251 (no hypocotyls) examples. During the hypocotyl detection stage, the sliding window
252 approach ²⁷ is used to perform an exhaustive search for hypocotyls. Finally, by keeping
253 the highest scored windows as true positives, polynomial regression is used to define a
254 curve that passes through all the detected hypocotyls. Although the user can manually
255 insert the location of the hypocotyls, this curve enables the position of undetected
256 hypocotyls to be estimated, and thus corrects the curve tracing. The intersection between
257 the hypocotyl detection curve and each root is used to define the root start point.

258 We first evaluated our hypocotyl detection process in terms of different hypocotyl
259 detection models. Both the precision-recall curve (Fig. 5b) and the number of false
260 positives per image (FPPI; Fig. 5c) were calculated for three different models that differ
261 in the type of feature they use for describing hypocotyls: only color information, only
262 appearance information (via HOG features), or both types of information (HOG + color).

263 Upon analyzing the precision-recall curve of each model, we found the HOG + color
264 model to be the most robust (Fig. 5b). In the case of FPPI, the lowest miss rate was also
265 found when using the HOG + color model (Fig. 5c). These results indicate that when
266 considering both color and appearance (i.e., the HOG + color model), more hypocotyls
267 are identified than when using only one of the features. Thus, this validates our MyROOT
268 method because it incorporates both HOG and color information.

269 Next, we evaluated the influence of different regression curve models on the root
270 measurement refinement used to set up the limits of individual roots (Fig. 5d). To create
271 these curves, a regression upon the detected hypocotyls was performed. In order to define
272 which regression model gives the better fit, we tested different polynomial models that
273 were evaluated in terms of the average distance (in pixels) between the real hypocotyl
274 position and the point of intersection between the root and the regression curve (Fig. 5d).
275 The results indicate that when using a hypocotyl regression curve of order 4, a good
276 balance between accuracy and flexibility that is able to account for small changes in
277 hypocotyl position is reached. As such, we chose to employ this regression curve in our
278 software.

279

280 **DISCUSSION**

281 The advent of root imaging and phenotyping has aided in the understanding not only of
282 plant organogenesis and development, but also of plant adaptation to changing
283 environments¹⁹. Here, we present MyROOT, a novel software for accurately measuring
284 root length from images of Arabidopsis seedlings that are grown vertically in Petri dishes.
285 In addition to its simple image acquisition method, this software minimizes user
286 intervention through the automatic detection of the scale, root tips and hypocotyls.
287 Compared to other available root software such as WinRhizo²⁸ or GROWSCREEN-Root
288²⁹, which require specialized imaging equipment such as scanners or infrared light,
289 MyROOT merely uses a standard digital camera.

290 One of the novel aspects of this software compared with other existing methods such as
291 ImageJ and RootTrace²³ is that MyROOT has been trained to automatically identify
292 hypocotyls, the shoot-root junction and the root tip of each seedling. Such automated
293 identification is necessary for minimizing the manual intervention of the user and as such,
294 the time dedicated to the root measurement task. In addition, MyROOT is also able to
295 identify hypocotyls of different sizes and morphologies, an aspect that also makes it
296 suitable for the phenotypic analysis of mutants or of plants grown in different conditions.
297 Furthermore, in exceptional cases where the software might be unable to automatically
298 recognize hypocotyls, they can actually be manually indicated by the user. In this way,
299 we have designed MyROOT as a versatile tool that can be used in a wide range of
300 developmental studies, including analyses of seedlings at different developmental stages
301 and under different conditions.

302 MyROOT is a modularly designed software. It consists of a group of specialized
303 algorithms able to detect and analyze the measuring tape, detect the roots, track the roots
304 in a bottom-up fashion, and detect the hypocotyls. Therefore, any improvement to any of
305 these components, or new algorithms for the determination of other features, can be easily
306 included in subsequent versions of MyROOT. Examples of future improvements that
307 could be included are the development of daily growth-monitoring algorithms that permit
308 the detection of abnormal root growth patterns, the analysis of root system architecture
309 beyond the primary root, and the identification of hypocotyls from other plant species. In
310 the future, upgraded versions of our software could consist of a completely automatic
311 operation connected to high-throughput facilities for massive root phenotyping.

312

313 **CONCLUSION**

314 MyROOT is a software capable of semi-automatically measuring the length of the
315 primary root of *Arabidopsis* seedlings. It automatically recognizes the scale of the image,
316 and detects the hypocotyls and root tips from young seedlings growing vertically in agar
317 plates. This information is then used to accurately calculate the root length of each
318 individual plant. This software was designed in such a way that only a simple image of
319 the plate is required for analysis. Importantly, MyROOT is even able to recognize
320 hypocotyls of different ages and morphologies, and can thus be applied in a large range
321 of experiments.

322 Here, our validation experiments demonstrate the high precision of measurements made
323 with MyROOT, thereby proving that this software can be used within the research
324 community to perform high-throughput experiments in a less time-consuming manner.

325

326 **MATERIAL AND METHODS**

327 **Plant material and growth conditions**

328 Wild type Col-0 *Arabidopsis thaliana* seeds were surface sterilized with a 5-min
329 incubation in 1.5% sodium hypochlorite, followed by five washes in distilled sterile
330 water. Seeds were stratified for 48 h at 4°C in the dark to synchronize germination. Seeds
331 were sown in 12x12-cm plates containing ½ Murashige and Skoog (MS) medium without
332 sucrose and supplemented with vitamins (0.5MS-). Seeds were distributed individually
333 in the plate in two rows with around 15 seeds per row. The plates were incubated for 3 to
334 8 days vertically oriented under long day conditions (16 hours of light and 8 of hours
335 dark) at 22°C and 60% relative humidity.

336 **Plant Imaging and computer settings**

337 Images were taken with a D7000 Nikon camera. The pre-defined image acquisition
338 conditions consist of placing the camera 50 cm above the plate with an illuminated
339 support and the following settings: aperture 13, shutter speed 10, ISO 100 and Zoom x35.
340 The plates were placed face down on a black surface and with a ruler (at least 1 cm long)
341 horizontally positioned on top (Fig. S1). The images were saved in JPEG format (size
342 between 2.5 and 2.7 MB per image).

343 MyROOT and ImageJ were run in a Intel® Core™ i7-6700 CPU computer.

344 **Hypocotyl detection model**

345 The software was trained to identify hypocotyls by using 1,259 positive examples
346 (hypocotyls) and 7,915 background and negative examples (parts of the image that did
347 not contain hypocotyls). The positive samples correspond to Col-0 wild type, *bri1-116*,
348 and a transgenic line overexpressing BRI1-GFP, which have morphologically different
349 hypocotyls as shown in ¹¹.

350 **Algorithms**

351 MyROOT has been developed in Matlab (version 8.3.0.532. Natick, Massachusetts: The
352 MathWorks Inc., 2014). It will be made available to the plant sciences community
353 through the Plant Image Analysis website (plant-image-analysis.org; ³⁰) a standalone
354 executable application.

355

356 **ACKNOWLEDGMENTS**

357 We would like to thank Caño-Delgado Lab members for helping with the manual root
358 length measurements and comments on the manuscript. A.I.C-D. is a recipient of a
359 BIO2016-78955 grants from the Spanish Ministry of Economy and Competitiveness and
360 a European Research Council, ERC Consolidator Grant (ERC-2015-CoG – 683163). I.B-
361 P. is funded by the FPU15/02822 grant from the Spanish Ministry of Education, Culture
362 and Sport. D.B-E. is contracted with the BIO2016-78955 grant in the A.I.C-D laboratory.
363 CRAG is funded by “Severo Ochoa Programme” from Centers of Excellence in R&D
364 2016-2019 (SEV-2015-485 0533).

365

366 **AUTHOR CONTRIBUTIONS**

367 A.I.C-D. conceived the idea. A.G. and X.S. developed the algorithms for the method.
368 A.G., X.S., I.B-P. and D.B-E performed the validation experiments. I.B-P. and D.B-E.
369 acquired the dataset. X.S. and A.I.C-D. designed and supervised the study. I.B-P., A.G.
370 X.S. and A.I.C-D. wrote the manuscript.

371

372 **FIGURE LEGENDS**

373 **Figure 1. The graphical interface and steps of MyROOT.**

374 **(a)** The graphical user interface of MyROOT is organized into six sections: 1. Input image
375 information, 2. Root extraction parameters, 3. Hypocotyl detection parameters, 4. Manual
376 removal of roots, 5. Visualization of the image and the different detection steps, and 6.
377 Saving parameters. **(b)** The input image required for analysis is a picture of the square
378 plate in which the aligned seedlings are growing. By using information from this image,
379 MyROOT performs the following steps: **(c)** Identification of the ruler to determine the
380 scale (i.e., the equivalence between pixels and millimeters), **(d)** Root segmentation to
381 identify the seedlings, **(e)** Root tracking to measure the roots, **(f)** Hypocotyl detection to
382 identify the hypocotyls and separate them from the roots, and **(g)** Root measurement to
383 quantify the length of individual seedlings (i.e., the distance from the root tip to the end
384 of the hypocotyl).

385 **Figure 2. The ruler identification process.**

386 **(a)** MyROOT computes the vertical and horizontal profiles of the image to look for a
387 white patch. **(b)** The ruler is identified. **(c)** The area corresponding to the ruler is then
388 segmented into light and dark areas (binarization), for which black lines (dark areas) are
389 identified with high values and white areas with lower values. **(d)** A profile is generated
390 in which black lines are identified as peaks. **(e)** By using the distance between peaks, the
391 equivalence between pixels and millimeters is calculated.

392 **Figure 3. Root extraction method.**

393 **(a)** Colors are normalized in the area where roots are present, and white roots are detected.
394 **(b)** Segmentation is performed by applying a ridge detector. **(c)** Starting at the root tip,
395 the roots are tracked using a bottom-up approach. **(d)** Each root is measured using its
396 historical recorded tracking, and root length is calculated by taking into account the pixel-
397 millimeter equivalence.

398 **Figure 4. Validation of root length measurements.**

399 **(a)** Root length of 6-day-old Arabidopsis seedlings (3 plates, n=89). Measurements were
400 performed by three different people using either the ImageJ tool or MyROOT. **(b)** Root
401 length of Arabidopsis seedlings over 6 days (from 3 DAG to 8 DAG, n>116).
402 Measurements were performed using either ImageJ or MyROOT. Error bars indicate the

403 standard error. Seedlings that were not measured by MyROOT in at least 4 time points
404 were discarded.

405 **Figure 5. Hypocotyl detection method and validation.**

406 **(a)** Scheme of the hypocotyl detection method. A candidate window is defined as a square
407 area inside the image. In order to describe a candidate, appearance/shape (HOG) and color
408 information are extracted. Appearance information is extracted to calculate the gradient
409 of the image (i.e., the direction of the contours within the image at each pixel). Histograms
410 of Oriented Gradient (HOG) and the histograms of color are calculated over regular
411 spaced, non-overlapping cells inside the candidate window (forming the block
412 descriptor). Finally, all color/HOG cell histograms are concatenated to obtain the
413 candidate window description. **(b)** Precision-Recall curve for three different models of
414 hypocotyl detection (HOG, Color and HOG+Color). The curve is obtained by changing
415 the threshold that defines the frontier between positive and negative samples. For each
416 threshold, the precision (well classified ratio) and the recall (poor classified ratio) were
417 calculated. The area under the curve represents the robustness of the classifier, with a
418 higher value indicating greater robustness (a higher well classified ratio to poor classified
419 ratio over the entire range of the classifier). **(c)** False Positives Per Image (FPPI) curve
420 for three different models of hypocotyl detection (HOG, Color and HOG+Color). The
421 curve plots the miss rate against the FPPI. In this way, the average miss rate over a specific
422 FPPI range (1 to 10) represents the sensitivity of the classifier to not miss good samples
423 and keep the false positive ratio low. **(d)** The average distance in pixels between the real
424 hypocotyl position and the point of intersection between the root and the polynomial
425 regression curves, for polynomial regression curves of orders 1 to 6 and an extra model
426 including a sine component. Error bars indicate the standard error.

427 **Supplementary Figure 1.** Laboratory setup for taking pictures of the plates. The image
428 shows the position of the lights, the camera and the plate to be analyzed, all positioned
429 over a black surface.

430 **Supplementary Figure 2.** Evaluation of the time required to measure root length. Time
431 (in seconds) required for three different scientists to measure the root length of two
432 different plates containing one and two rows of seedlings respectively. The measurements
433 were done with MyROOT and ImageJ. Error bars indicate the standard error.

434 **BOX 1: Installation guide for MyROOT software.**

435 **BOX 2: Brief user guide for MyROOT software.**

436

437 **REFERENCES**

- 438 1 Kuijken, R. C., van Eeuwijk, F. A., Marcelis, L. F. & Bouwmeester, H. J. Root phenotyping:
439 from component trait in the lab to breeding. *Journal of experimental botany* **66**, 5389-
440 5401, doi:10.1093/jxb/erv239 (2015).
- 441 2 Dolan, L. *et al.* Cellular organisation of the Arabidopsis thaliana root. *Development* **119**,
442 71-84 (1993).
- 443 3 Ishikawa, H. & Evans, M. L. Specialized zones of development in roots. *Plant physiology*
444 **109**, 725-727 (1995).
- 445 4 Iyer-Pascuzzi, A., Simpson, J., Herrera-Estrella, L. & Benfey, P. N. Functional genomics of
446 root growth and development in Arabidopsis. *Current opinion in plant biology* **12**, 165-
447 171, doi:10.1016/j.pbi.2008.11.002 (2009).
- 448 5 Beemster, G. T. & Baskin, T. I. Analysis of cell division and elongation underlying the
449 developmental acceleration of root growth in Arabidopsis thaliana. *Plant physiology*
450 **116**, 1515-1526 (1998).
- 451 6 Verbelen, J. P., De Cnodder, T., Le, J., Vissenberg, K. & Baluska, F. The Root Apex of
452 Arabidopsis thaliana Consists of Four Distinct Zones of Growth Activities: Meristematic
453 Zone, Transition Zone, Fast Elongation Zone and Growth Terminating Zone. *Plant*
454 *signaling & behavior* **1**, 296-304 (2006).
- 455 7 Takatsuka, H. & Umeda, M. Hormonal control of cell division and elongation along
456 differentiation trajectories in roots. *Journal of experimental botany* **65**, 2633-2643,
457 doi:10.1093/jxb/ert485 (2014).
- 458 8 van den Berg, C., Willemsen, V., Hendriks, G., Weisbeek, P. & Scheres, B. Short-range
459 control of cell differentiation in the Arabidopsis root meristem. *Nature* **390**, 287-289,
460 doi:10.1038/36856 (1997).
- 461 9 Jürgens, G., Mayer, U., Busch, M., Lukowitz, W. & Laux, T. Pattern formation in the
462 Arabidopsis embryo: a genetic perspective. *Philosophical transactions of the Royal*
463 *Society of London. Series B, Biological sciences* **350**, 7, doi:10.1098/rstb.1995.0132
464 (1995).
- 465 10 Benfey, P. N. *et al.* Root development in Arabidopsis: four mutants with dramatically
466 altered root morphogenesis. *Development* **119**, 57-70 (1993).
- 467 11 Gonzalez-Garcia, M. P. *et al.* Brassinosteroids control meristem size by promoting cell
468 cycle progression in Arabidopsis roots. *Development* **138**, 849-859,
469 doi:10.1242/dev.057331 (2011).
- 470 12 Potuschak, T. *et al.* EIN3-dependent regulation of plant ethylene hormone signaling by
471 two arabidopsis F box proteins: EBF1 and EBF2. *Cell* **115**, 679-689 (2003).
- 472 13 Hauser, M. T., Morikami, A. & Benfey, P. N. Conditional root expansion mutants of
473 Arabidopsis. *Development* **121**, 1237-1252 (1995).
- 474 14 Cano-Delgado, A. I., Metzclaff, K. & Bevan, M. W. The eli1 mutation reveals a link between
475 cell expansion and secondary cell wall formation in Arabidopsis thaliana. *Development*
476 **127**, 3395-3405 (2000).
- 477 15 Mouchel, C. F., Briggs, G. C. & Hardtke, C. S. Natural genetic variation in Arabidopsis
478 identifies BREVIS RADIX, a novel regulator of cell proliferation and elongation in the root.
479 *Genes & development* **18**, 700-714, doi:10.1101/gad.1187704 (2004).
- 480 16 Ubeda-Tomas, S. *et al.* Root growth in Arabidopsis requires gibberellin/DELLA signalling
481 in the endodermis. *Nature cell biology* **10**, 625-628, doi:10.1038/ncb1726 (2008).

- 482 17 Gonzalez-Garcia, M. P. *et al.* Single-cell telomere-length quantification couples telomere
483 length to meristem activity and stem cell development in Arabidopsis. *Cell reports* **11**,
484 977-989, doi:10.1016/j.celrep.2015.04.013 (2015).
- 485 18 Pfister, A. *et al.* A receptor-like kinase mutant with absent endodermal diffusion barrier
486 displays selective nutrient homeostasis defects. *eLife* **3**, e03115,
487 doi:10.7554/eLife.03115 (2014).
- 488 19 Lobet, G. Image Analysis in Plant Sciences: Publish Then Perish. *Trends in plant science*
489 **22**, 559-566, doi:10.1016/j.tplants.2017.05.002 (2017).
- 490 20 Yazdanbakhsh, N. & Fisahn, J. High-throughput phenotyping of root growth dynamics.
491 *Methods Mol Biol* **918**, 21-40, doi:10.1007/978-1-61779-995-2_3 (2012).
- 492 21 Slovak, R. *et al.* A Scalable Open-Source Pipeline for Large-Scale Root Phenotyping of
493 Arabidopsis. *The Plant cell* **26**, 2390-2403, doi:10.1105/tpc.114.124032 (2014).
- 494 22 Clark, R. T. *et al.* High-throughput two-dimensional root system phenotyping platform
495 facilitates genetic analysis of root growth and development. *Plant, cell & environment*
496 **36**, 454-466, doi:10.1111/j.1365-3040.2012.02587.x (2013).
- 497 23 French, A., Ubeda-Tomas, S., Holman, T. J., Bennett, M. J. & Pridmore, T. High-
498 throughput quantification of root growth using a novel image-analysis tool. *Plant*
499 *physiology* **150**, 1784-1795, doi:10.1104/pp.109.140558 (2009).
- 500 24 Remmler, L., Clairmont, L., Rolland-Lagan, A. G. & Guinel, F. C. Standardized mapping of
501 nodulation patterns in legume roots. *The New phytologist* **202**, 1083-1094,
502 doi:10.1111/nph.12712 (2014).
- 503 25 Otsu, N. A Threshold Selection Method from Gray-Level Histograms. *IEEE Transactions*
504 *on Systems, Man, and Cybernetics* **9**, 5, doi:10.1109/tsmc.1979.4310076 (1979).
- 505 26 Dalal, N. & Triggs, B. Histograms of Oriented Gradients for Human Detection. *Computer*
506 *Society Conference on Computer Vision and Pattern Recognition* **1**, 8,
507 doi:10.1109/CVPR.2005.177 (2005).
- 508 27 Glumov. Detection of objects on the image using a sliding window mode. *Optics & Laser*
509 *Technology* **27**, 9 (1995).
- 510 28 Arsenault, J., Poulcur, S., Messier, C. & Guay, R. Winrhizo: A root measuring system with
511 a unique overlap correction method. *HortScience* **30** (1995).
- 512 29 Nagel, K. *et al.* Temperature responses of roots: impact on growth, root system
513 architecture and implications for phenotyping. *Functional Plant Biology* **36**, 12 (2009).
- 514 30 Lobet, G., Draye, X. & Perilleux, C. An online database for plant image analysis software
515 tools. *Plant methods* **9**, 38, doi:10.1186/1746-4811-9-38 (2013).

516

517

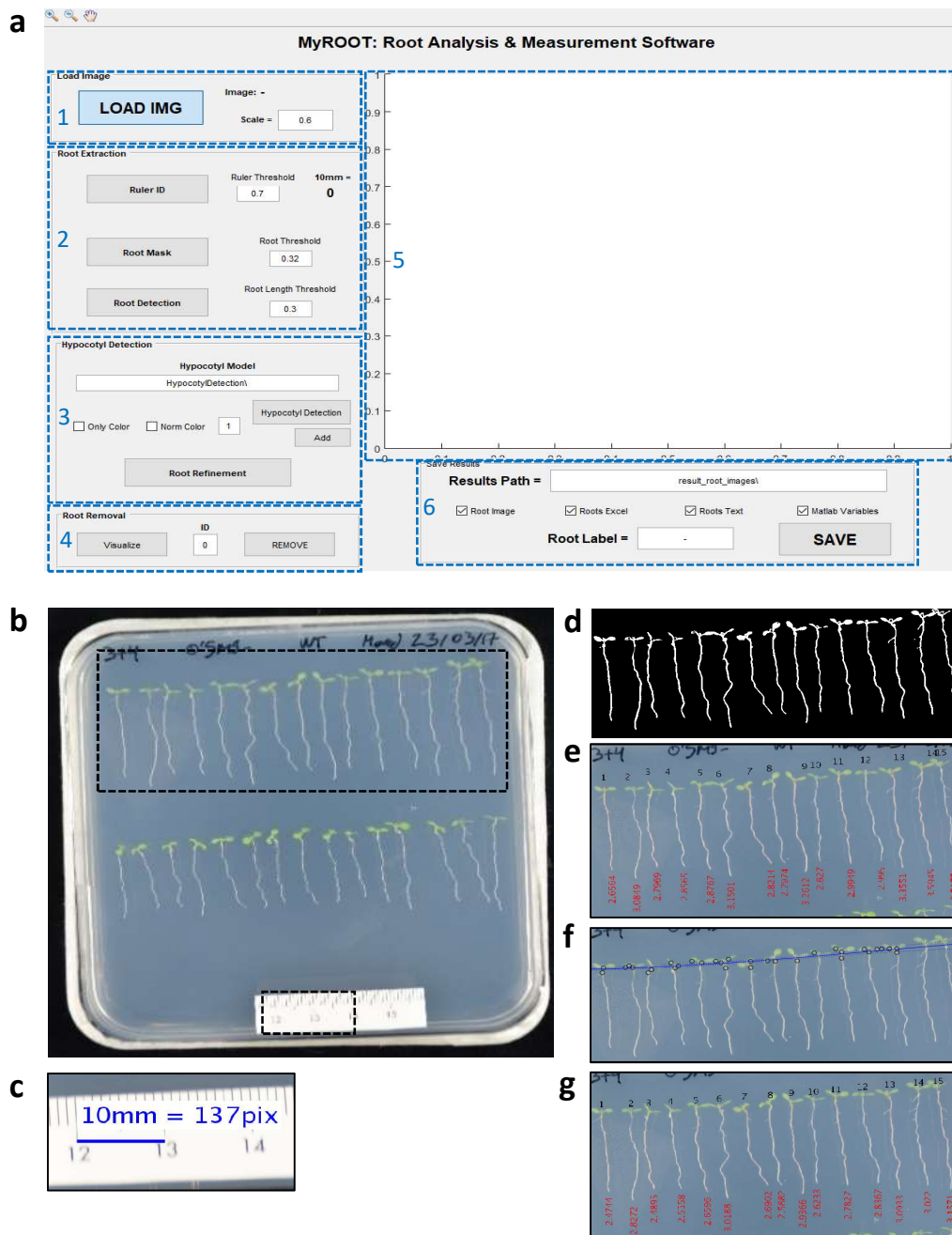


Figure 1. The graphical interface and steps of MyROOT.

(a) The graphical user interface of MyROOT is organized into six sections: 1. Input image information, 2. Root extraction parameters, 3. Hypocotyl detection parameters, 4. Manual removal of roots, 5. Visualization of the image and the different detection steps, and 6. Saving parameters. (b) The input image required for analysis is a picture of the square plate in which the aligned seedlings are growing. By using information from this image, MyROOT performs the following steps: (c) Identification of the ruler to determine the scale (i.e., the equivalence between pixels and millimeters), (d) Root segmentation to identify the seedlings, (e) Root tracking to measure the roots, (f) Hypocotyl detection to identify the hypocotyls and separate them from the roots, and (g) Root measurement to quantify the length of individual seedlings (i.e., the distance from the root tip to the end of the hypocotyl).

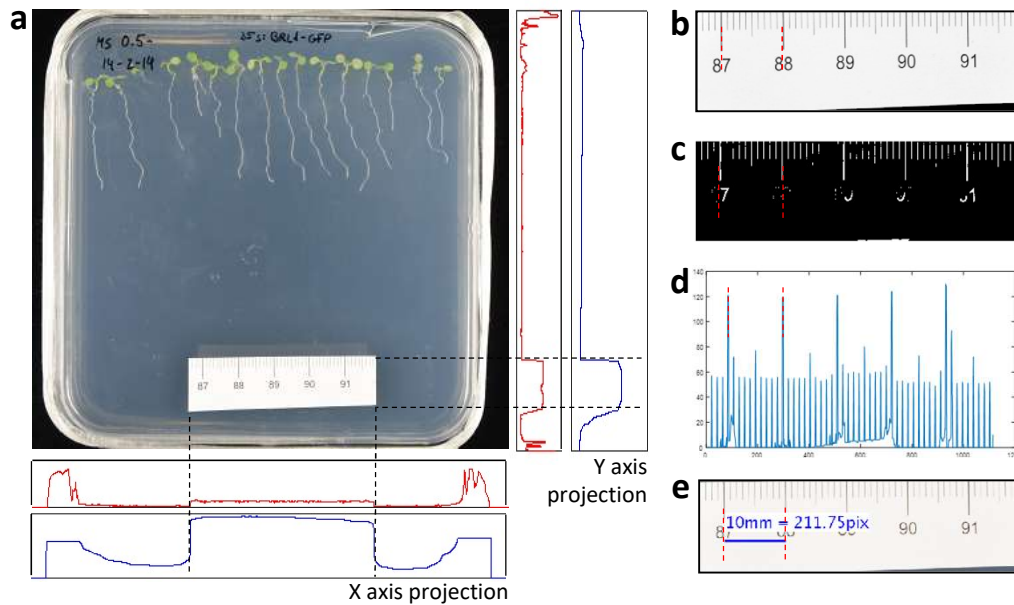


Figure 2. The ruler identification process.

(a) MyROOT computes the vertical and horizontal profiles of the image to look for a white patch. (b) The ruler is identified. (c) The area corresponding to the ruler is then segmented into light and dark areas (binarization), for which black lines (dark areas) are identified with high values and white areas with lower values. (d) A profile is generated in which black lines are identified as peaks. (e) By using the distance between peaks, the equivalence between pixels and millimeters is calculated.

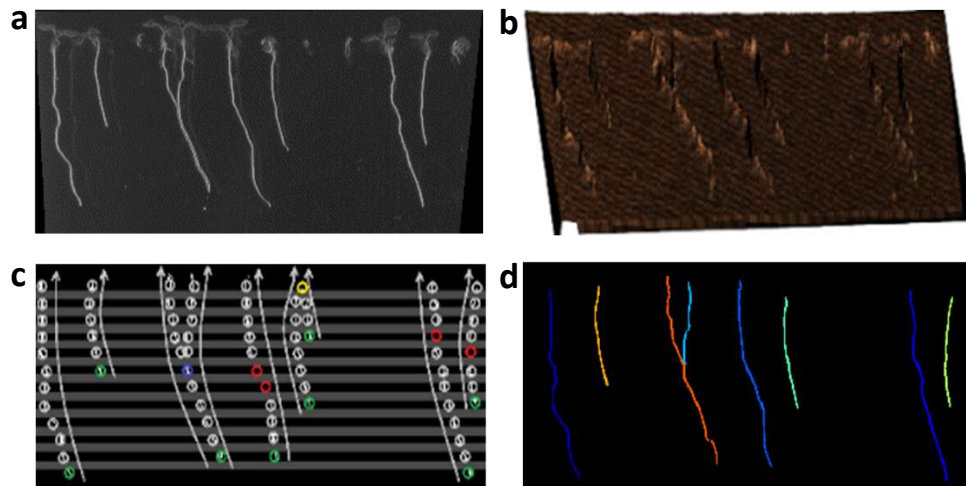


Figure 3. Root extraction method.

(a) Colors are normalized in the area where roots are present, and white roots are detected. (b) Segmentation is performed by applying a ridge detector. (c) Starting at the root tip, the roots are tracked using a bottom-up approach. (d) Each root is measured using its historical recorded tracking, and root length is calculated by taking into account the pixel-millimeter equivalence.

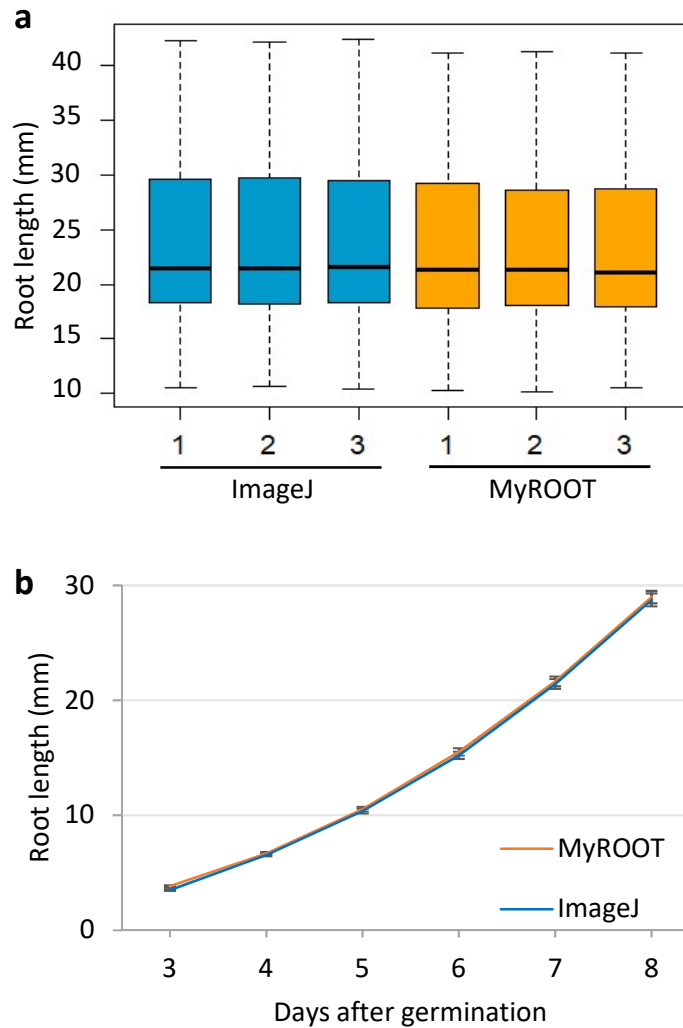


Figure 4. Validation of root length measurements.

(a) Root length of 6-day-old Arabidopsis seedlings (3 plates, n=89). Measurements were performed by three different people using either the ImageJ tool or MyROOT. **(b)** Root length of Arabidopsis seedlings over 6 days (from 3 DAG to 8 DAG, n>116). Measurements were performed using either ImageJ or MyROOT. Error bars indicate the standard error. Seedlings that were not measured by MyROOT in at least 4 time points were discarded.

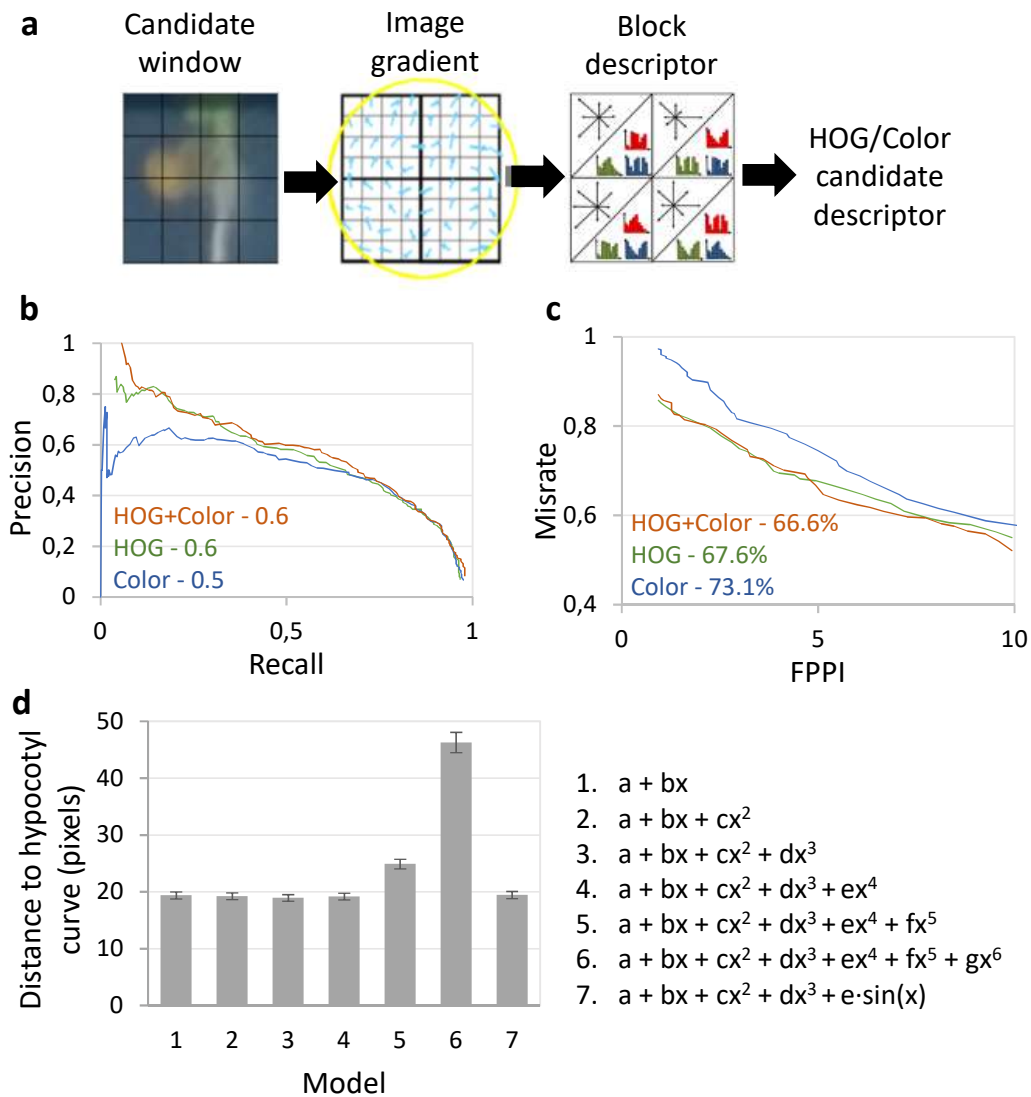


Figure 5. Hypocotyl detection method and validation.

(a) Scheme of the hypocotyl detection method. A candidate window is defined as a square area inside the image. In order to describe a candidate, appearance/shape (HOG) and color information are extracted. Appearance information is extracted to calculate the gradient of the image (i.e., the direction of the contours within the image at each pixel). Histograms of Oriented Gradient (HOG) and the histograms of color are calculated over regular spaced, non-overlapping cells inside the candidate window (forming the block descriptor). Finally, all color/HOG cell histograms are concatenated to obtain the candidate window description. **(b)** Precision-Recall curve for three different models of hypocotyl detection (HOG, Color and HOG+Color). The curve is obtained by changing the threshold that defines the frontier between positive and negative samples. For each threshold, the precision (well classified ratio) and the recall (poor classified ratio) were calculated. The area under the curve represents the robustness of the classifier, with a higher value indicating greater robustness (a higher well classified ratio to poor classified ratio over the entire range of the classifier). **(c)** False Positives Per Image (FPPI) curve for three different models of hypocotyl detection (HOG, Color and HOG+Color). The curve plots the miss rate against the FPPI. In this way, the average miss rate over a specific FPPI range (1 to 10) represents the sensitivity of the classifier to not miss good samples and keep the false positive ratio low. **(d)** The average distance in pixels between the real hypocotyl position and the point of intersection between the root and the polynomial regression curves, for polynomial regression curves of orders 1 to 6 and an extra model including a sine component. Error bars indicate the standard error.

BOX 1: Installation guide for MyROOT software

1. Execute MyAppInstaller_mcr.exe.
2. In the Root Analysis Installer window press the *Next* button.
3. In the Installation Options window select the folder where you wish to install the software. By default, the selected folder is C:\Program Files\La Salle – Universidad Ramon Llull\Root_Analysis.
4. Mark the option *Add a shortcut to the desktop*.
5. Press the *Next* button.
6. In the Required Software window select the installation folder for the MATLAB Runtime (by default C:\Program Files\MATLAB\MATLAB Runtime)
7. Press the *Next* button.
8. In the License Agreement window mark the option *Yes*.
9. Press the *Next* button.
10. In the Confirmation window press the *Install* button.
11. Copy the HypocotylDetection folder to the Desktop (this folder is in the same folder as the .exe file used for the installation).
12. Open the software by pressing in the MyROOT Desktop icon.

BOX 2: Brief user guide for MyROOT software

1. Open the software in a PC.
2. Select and load the image to process by pressing the *LOAD IMG* button. Enter an image resize factor between 0 and 1 in the Scale edit box to reduce the size of the image and speed up the processing of high-resolution images.
3. Obtain the pixels-to-millimeters scale factor by pressing the *Ruler ID* button. If needed, edit the Ruler Threshold value to modify the sensitivity of the ruler detector and repeat step 3.
4. Start the root segmentation process by pressing the *Root Mask* button. Select the area where the roots are present by clicking in the image. Double click in one of the vertex to start generating the mask. In case the result is not satisfactory (e.g., over-segmented roots), modify the sensitivity factor in the Root Threshold edit box and repeat step 4.
5. Enter a value in the Root Length Threshold box to indicate the minimum percentage with respect to the longest root to be measured.
6. Start the root tracking and measurement process by pressing the *Root Detection* button.
7. Enter the path of the files containing the pre-trained hypocotyl detection models in the Hypocotyl Model Path edit box.
8. Optionally, to perform hypocotyl detection based on color descriptors only, check the *Only Color* checkbox, and to conduct a channel-wise color normalization process check the *Norm Color* checkbox.
9. Optionally, modify the threshold of the linSVM classifier by modifying the value in the edit box located next to the Hypocotyl Detection button.
10. Start the hypocotyl detection process by pressing the *Hypocotyl Detection* button.
11. If some of the hypocotyls were undetected, insert them manually by using the *Add* button. Press the *Enter* key and press the *Root Refinement* button to update root length measurements.
12. Remove the undesired roots from the measurement by typing the root identifier in the ID edit box and pressing the *Remove* button. Press the *Visualize* button to refresh the image presented on MyROOT's visualization canvas.
13. Enter the path where you would like the results to be stored in the Results Path edit box.
14. Choose the type of data you want to save by checking the corresponding checkboxes.
15. Optionally, type an identification suffix that will be appended to the stored file names via the Root Label edit box.
16. Save the results by pressing the *SAVE* button.